Journal of Power Sources 270 (2014) 627–633

Contents lists available at ScienceDirect

Journal of Power Sources

journal homepage: www.elsevier.com/locate/jpowsour

Phosphoric acid distribution and its impact on the performance of polybenzimidazole membranes

Florian Mack [a], Stefan Heissler [b], Ruben Laukenmann [a], Roswitha Zeis [a, *]

[a] Karlsruhe Institute of Technology (KIT), Helmholtz Institute Ulm (HIU), D-89081 Ulm, Germany
[b] Karlsruhe Institute of Technology (KIT), Institute of Functional Interfaces (IFG), D-76344 Eggenstein-Leopoldshafen, Germany

HIGHLIGHTS

- Not only doping degree but also doping time defines the conductivity of the membrane.
- Prolonged doping time achieves uniform phosphoric acid distribution in the membrane.
- Confocal Raman microscopy visualizes acid distribution depending on the doping time.
- Homogenous phosphoric acid distribution reduces acid migration out of the membrane.
- Doping time and temperature have to be optimised for each type of polymer membrane.

GRAPHICAL ABSTRACT

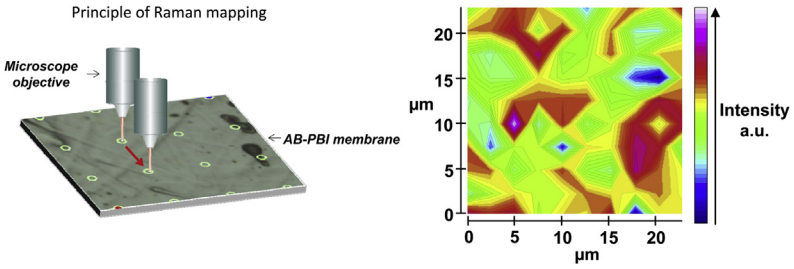

ARTICLE INFO

Article history:
Received 10 February 2014
Received in revised form
4 June 2014
Accepted 5 June 2014
Available online 1 August 2014

Keywords:
HT-PEM
PBI doped with phosphoric acid
Confocal Raman microscopy
Membrane conductivity
Phosphoric acid distribution
PBI – phosphoric acid interaction

ABSTRACT

Phosphoric acid doped polybenzimidazole (PBI) is the most common membrane material for high-temperature polymer electrolyte membrane fuel cells (HT-PEMFC). The PBI membrane is usually doped by immersion in hot phosphoric acid. Immersion time and acid temperature affect the doping level of the membrane. In this work we studied the influence of doping time and temperature on the ex-situ and in-situ proton conductivities of poly (2, 5-benzimidazole) (AB-PBI) membranes as well as the fuel cell performance. Confocal Raman microscopy was employed to spatially resolve the acid distribution within the AB-PBI membranes. Therefore the interactions between the basic nitrogen-sides of the AB-PBI polymer and the phosphoric acid protons were investigated. We found that membranes with a 6 h doping time had significantly higher proton conductivity than those doped for only 3 h. In terms of absolute acid up-take, however, the difference was rather small. This result shows that the doping level alone does not define the conductivity of the membrane. The conductivity is also influenced by the micro acid distribution within the membrane. Highest membrane conductivity and fuel cell performance with fumapem AM cross-linked membranes were achieved with a doping time of 6 h and a doping temperature of 120 °C.

1. Introduction

The HT-PEMFC operates at temperatures from 140 °C to 200 °C and requires high membrane conductivity in this temperature range. The HT-PEMFC performance benefits from high working

* Corresponding author.
E-mail address: roswitha.zeis@kit.edu (R. Zeis).

http://dx.doi.org/10.1016/j.jpowsour.2014.06.171
0378-7753/

temperatures due to faster electrode kinetics and a higher tolerance to impurities like carbon monoxide (CO) [1,2]. Perfluorosulfonic acid polymers like Nafion, the most common membrane material for low-temperature PEMFCs, rely on hydration of the membrane to ensure high proton conductivity at elevated temperatures [3,4]. Many hydrocarbon polymers were investigated as alternatives to Nafion for HT-PEMFC applications [5] and one of the most promising candidates is phosphoric acid doped Poly[2,2-(m-phenylene)-5,5-bibenzimidazole] (PBI) [6,7].

PBI is an aromatic heterocyclic polymer with good chemical resistance and high mechanical strength [8]. To achieve adequate proton conductivity for fuel cell operation, however, PBI needs to be doped with acid because of its low intrinsic conductivity. The doped membranes show high conductivity at low humidified conditions [9] and low gas crossover [10]. A promising PBI derivate is AB-PBI [11–13] which can be easily synthesized from a single cheap monomer [14].

Usually phosphoric acid is used as the doping agent for PBI membranes due to the high conductivity of phosphoric acid doped membranes compared with other acids as doping agents [15]. Membrane conductivity strongly depends on the amount of acid inside the membrane [16], which depends on the acid concentration [17] and the doping time [18]. The membrane conductivity plays a key role for the fuel cell performance and therefore a high amount of acid in the membrane (doping level) is preferred. However, apart from the total amount of phosphoric acid inside the membrane, the interactions between the acid molecules and the N-sides of the AB-PBI are important to prevent acid leakage from the membrane into the electrodes and gas diffusion layers (GDL) during fuel cell operation.

These interactions can be observed with Raman spectroscopy [18]. There are only a limited number of studies on PBI with Raman spectroscopy despite the fact that Raman measurements are fast and non-destructive [19], which further enables confocal Raman imaging with a fairly high in-plane spatial resolution [20]. Recently, AB-PBI membranes doped with different amounts of phosphoric acid were investigated with Raman spectroscopy and the characteristic bands were assigned [21]. Several PBI derivates were studied with this method [22], [23]. However, to our knowledge, spatially resolved confocal Raman microscopy had not been used to study phosphoric acid doped AB-PBI membranes before.

In this study, we report the effects of the doping time and acid temperature on the ex-situ membrane conductivity, the fuel cell performance, and the cell resistance (which is mainly determined by the in-situ membrane conductivity). The interactions between phosphoric acid and the AB-PBI membrane were visualized with confocal Raman microscopy.

2. Experimental

2.1. Membrane doping and gas diffusion electrode preparation

AB-PBI membranes (fumapem AM cross-linked, Fuma-Tech) were doped with phosphoric acid by immersion in concentrated phosphoric acid (85%, Carl Roth) at different temperatures in the range of 80–140 °C for up to 7 h to achieve various doping levels (Fig. 2). The temperature was controlled by a dry bath thermostat (Boekel scientific) and the amount of acid in the membrane was determined gravimetrically. The surface of the membranes was carefully blotted with paper to remove phosphoric acid on the surface. The estimated error of this measurement is less than 10%.

For the gas diffusion electrode (GDE) catalyst suspensions ("catalyst inks") containing water (Millipore), isopropanol, PTFE solution (60%, 3 M), and 20% Pt/C catalyst (Heraeus) were used. The catalyst ink was sprayed in multiple layers directly onto the microporous layer of the GDL (H2315 C2, Freudenberg) at a substrate temperature of 80 °C. For this study, the catalyst loading was kept constant at 1 mg cm^{-2}, which was gravimetrically determined and the GDEs had a PTFE content of 10% by weight. A detailed description of the GDE preparation was described in Ref. [24].

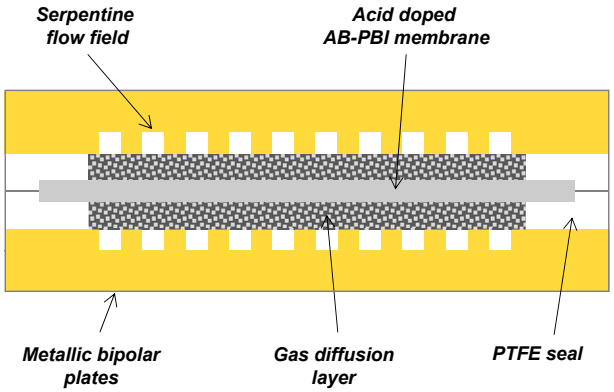

Fig. 1. Full cell setup layout for impedance measurements.

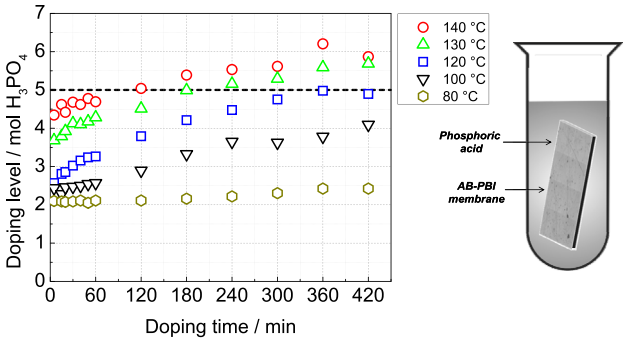

Fig. 2. Doping process of an AB-PBI membrane in hot phosphoric acid at various temperatures. The weight increase of AB-PBI membranes correlates with the sojourn time in the phosphoric acid (left). Illustration of an AB-PBI membrane immersed in acid (right).

2.2. Electrochemical characterization

The membrane electrode assemblies (MEAs) were prepared by placing the GDEs in direct contact with the doped AB-PBI membranes in single cells without hot-pressing (Fig. 1). The single cells with an active area of 4 cm^2 included gaskets (PTFE from Bohlender), sub-gaskets (PEEK from Victrex), metallic bipolar plates with single serpentine flow-fields (1 mm × 1 mm in dimension), and aluminum plates equipped with heating cartridges. The MEAs were compressed by circa 30% of the total thickness of individual components to maintain a constant contact pressure. The cell performance was studied at 160 °C and ambient pressure using dry hydrogen and air as reactants. Stoichiometric mass flows of hydrogen ($\lambda = 1.4$) and air ($\lambda = 2$) were used for current densities equal to or above 200 mA cm^{-2}. Gas flows were fixed for current densities below 200 mA cm^{-2}. Polarization curves were recorded by increasing the current density stepwise from zero (open circuit) up to 800 mA cm^{-2} or until the cell voltage dropped below 300 mV. Cell internal resistances were determined by measuring AC impedances at 1 kHz with an MR 2212 W impedance meter (Schuetz Meβtechnik).

The membrane ex-situ conductivity was measured with the same hardware except that the cell was not supplied with reactant

gases. For this purpose, the phosphoric acid doped AB-PBI membranes were placed between two non-teflonized GDLs (H2315 from Freudenberg) without catalyst layers. They were saturated with phosphoric acid to avoid acid leakage from the membranes during the measurement.

2.3. Confocal Raman microscopy

Confocal Raman microscopy was applied to determine the acid distribution in the membranes. The measurements were carried out using a Bruker Senterra (Bruker Optics, Ettlingen, Germany) Raman Microscope equipped with a red laser diode, $\lambda = 785$ nm, operated at 50 mW output power. The laser power was optimized to avoid any photo bleaching or damages of the membranes by the excitation energy.

For focusing of the laser beam as well as for collection of the backscattered light a 20× Olympus (Olympus, Tokyo, Japan) MPLAN objective, NA 0.45, was used. To achieve good signal/noise ratios the integration time was set from 10 to 30 s. At each measurement point at least four coadditons were collected. For each sample an area of 23 × 23 μm was mapped. Over this area 10 × 10 equidistant measurement points were set, which resulted in a lateral step size of 2.3 μm. The samples were mounted in a specially designed sample holder made from PVC to ensure a flat membrane in the focal plane along the whole mapping area. During data acquisition, the samples were kept in a dry chamber to prevent any interaction between the air humidity and the phosphoric acid. Spectra were measured in the range of 100–3200 cm^{-1} and the spectral resolution was 9 cm^{-1}. Data were acquired and evaluated using the Bruker OPUS® 7.2 software.

3. Results and discussion

3.1. Doping level and ex-situ conductivity

Fig. 2 shows the doping level of the AB-PBI membranes, which is the number of phosphoric acid molecules per repeating unit of AB-PBI, for various doping temperatures as a function of doping time. At 80 °C an initial doping level of 2 was observed, however the acid uptake only increased slightly with prolonged doping time. The energy input at this temperature is not high enough to decrease the intermolecular forces between the AB-PBI molecular chains which were strengthened by cross-linking of the AB-PBI and allow the phosphoric acid to penetrate the whole polymer.

At 100 °C a sigmoid shape of the uptake curve was observed. The plane parts of the doping curve at 100 °C appear similar to the doping curve at 80 °C and the strong increase between 1 and 4 h as well as after 6 h is comparable to the mainly diffusion controlled doping process at higher temperatures. Therefore we assume that primarily the easier accessible outer regions of the membrane are doped with phosphoric acid and at prolonged immersion time also the inner regions of the membrane are soaked with phosphoric acid.

At doping levels above 5, the colorless phosphoric acid turned slightly into brown during the doping process which was also observed by the group of Bjerrum for the doping of PBI blend membranes at 130 °C [25]. This fact and the deterioration of the mechanical stability of the membranes at doping levels above 5 indicate polymer loss due to partially dissolution of the membrane which resulted in fast membrane degradation in the fuel cell. This effect was also observed for membranes doped at 100 °C for 20 h with a doping level of about 5. In contrast to the doping of PBI [26], the final acid uptake of cross-linked AB-PBI strongly depends on the doping temperature.

Fig. 3 shows the temperature dependent resistance of membranes doped at 120 °C for various times. It was determined with a full cell setup for conductivity measurements as shown in Fig. 1. The ohmic resistances of the bipolar plates and the GDLs are very low and negligible. Due to the phosphoric acid saturated surrounding of the membrane, the migration of acid from the membrane into the GDL (the so called “acid leaching”) was prevented and the membrane conductivity was stable over time. The measured increase of conductivity with rising temperature had been observed before by other groups [1].

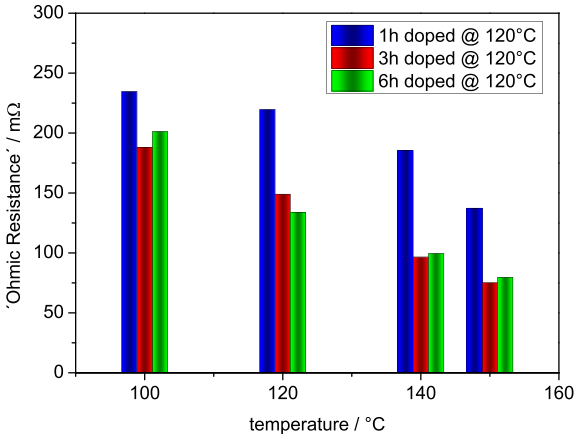

Fig. 3. Ex-situ conductivity measurements of AB-PBI membranes doped with phosphoric acid for 1 h, 3 h or 6 h.

At 100 °C, the ohmic resistance of the 1 h at 120 °C doped membrane is ca. 20% higher than that of longer doping durations of 3 and 6 h. At 120 °C, this difference increased to about 50%, and at 140–150 °C it was 80–90%. This can be qualitatively explained with the higher acid uptake of the membrane during longer doping periods. We note the amount of acid in the membrane increased by 30% (3 h) and 50% (6 h) compared with 1 h doping time (Fig. 2). However, the conductivities of the membranes with 3 and 6 h doping times were comparable over the entire temperature range from 100 to 150 °C, which does not directly correlate with the 15% higher amount of acid in the membrane doped for 6 h. The different temperature dependence of the membrane conductivity indicates that the activation energy of conduction is partially affected by the doping level. When the temperature is increased from 100 to 150 °C the resistance of the 1 h doped membrane decreases by a factor of 1.7 and the resistance of the membranes doped for 3 h and 6 h decreases by a factor of 2.7. Therefore we assume that the activation energy of conduction is higher with increasing doping level of the membrane. This result is in contrary to investigations of PBI membranes as described in Ref. [17]. However, due to the different doping behavior of AB-PBI and PBI and various experimental conditions, the results can not be directly compared.

3.2. In-situ conductivity

The influence of the doping time of the AB-PBI membranes on the in-situ conductivity was determined during the measurements of the fuel cell performance (Fig. 4). In contrast to the ex-situ measurements, no additional phosphoric acid was added to the GDL and a redistribution of the phosphoric acid inside the MEA was possible. This effect was enhanced by the generation of product water at the cathode, which tends to increase acid leaching. The in-situ resistance of the 1 h at 120 °C doped membrane was drastically higher than the corresponding ex-situ measurement (Fig. 3), and it was about 5 times higher than that of 3 h doping time at 120 °C. The phosphoric acid seems to leech out of the membrane into the GDEs and therefore increases the membrane resistance.

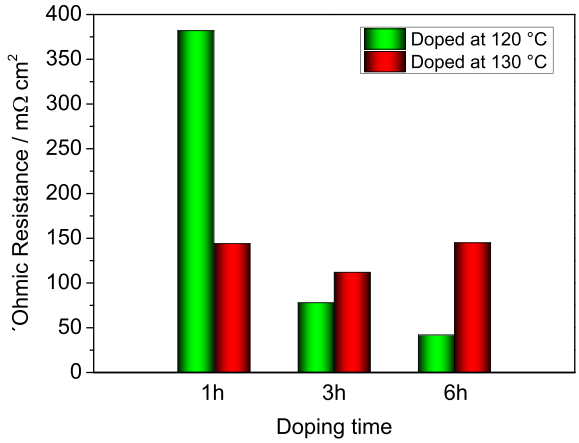

Fig. 4. In-situ conductivity of AB-PBI membranes dependent on the doping time and temperature. T = 160 °C, A = 4 cm^2, 1 mg Pt cm^{-2}, hydrogen/air with λ = 1.4/2, j = 200 mA cm^{-2}.

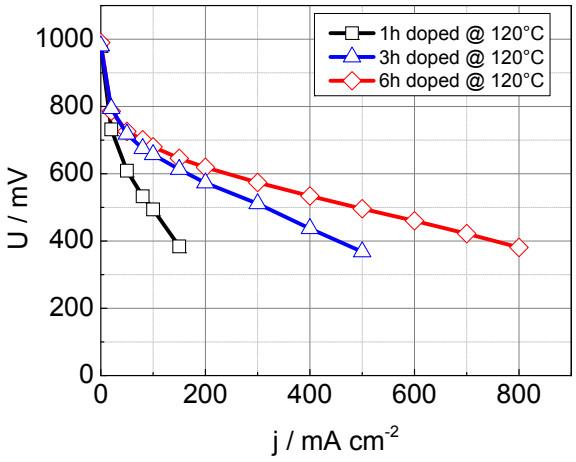

Fig. 5. Influence of the doping time of the AB-PBI membrane on the cell performance. Membranes were doped at 120 °C. T = 160 °C, A = 4 cm^2, 1 mg Pt cm^{-2}, hydrogen/air with λ = 1.4/2.

We assume that short doping times lead to a less uniform acid distribution in the membrane with a decreasing phosphoric acid amount from the surface to the middle of the membrane. At doping levels higher than 2, i.e. when the quantity of acid molecules is higher than the available basic sites of the polymer [27], free acid is present in the membrane. At short doping times, the free acid is primarily located at the exterior layers of the membrane because cross-linking of the AB-PBI increases the cohesion of the polymer backbone and therefore extends the required time for complete penetration of the membrane with phosphoric acid. Low acid content in the middle of the membrane increases the membrane resistance and a high acid content in the top layers of the membrane enhances acid leaching.

The membrane resistance with 6 h doping time at 120 °C decreased by half compared with doping time of 3 h, dropping below the ex-situ measurement value. Besides reduced acid leaching, we assume a positive impact of the product water from the cathode on the conductivity of the phosphoric acid in the membrane. This effect had been reported earlier for ex-situ measurements of the AB-PBI membrane conductivity as a function of relative humidity [1].

In contrast to the results for membranes doped at 120 °C, the lowest in situ resistance for membranes doped at 130 °C was achieved after 3 h doping time and a doping level of 5. Lower doping levels increase the resistance due to an insufficient amount of phosphoric acid in the membrane and higher doping levels are associated with partially dissolution of the polymer. The optimal doping level for the fumapem AM cross-linked membrane is 5, however it has to be optimized for each type of polymer as shown by doping studies for PBI blend [25] and PBI [26] membranes.

3.3. Cell performance

The phosphoric acid doped membranes with a doping temperature of 120 °C and different doping times were incorporated into MEAs and their performance was investigated in single cell tests (Fig. 5). The results are in accordance with the in-situ conductivity measurements. The open circuit voltages were comparable for all MEAs; however the MEA based on the 1 h doped membrane showed high ohmic losses and therefore an insufficient performance for fuel cell operation. The performance of the MEA based on the 3 h doped membrane is drastically higher. The MEA with the longest doping time of 6 h clearly demonstrated the best performance. The different performance of the MEAs is not only due to the ohmic resistances, but also caused by acid leaching from the membrane which leads to electrode flooding. The acid migration from the membrane to the electrodes not only decreases the membrane conductivity but also fills up the electrode pores with phosphoric acid, which impedes the reaction gas supply of the triple phase boundary and hinders the electrochemical reactions.

The MEA based on the 1 h doped membrane only achieved a peak power density of 58 mW cm^{-2}, which is quite low compared with the 3 h and 6 h doped membranes with peak power densities of 184 mW cm^{-2} and 305 mW cm^{-2}. The MEA with the 6 h doped membrane exhibits a higher performance than MEAs prepared in a similar manner (250 mW cm^{-2}) [28] due to improved electrode composition [29], but the performance of MEAs based on the 3 h doped membrane is still distinctly lower.

Membranes doped at 130 °C for 3 h reached the same doping level of 5 as membranes doped at 120 °C for 6 h. In order to determine the influence of the doping time on the performance regardless of the doping level, these membranes were incorporated into MEAs and evaluated in single cell tests (Fig. 6). However, only a peak power density of 145 mW cm^{-2} was achieved. This result can be correlated with the membrane resistance (Fig. 4) which is more

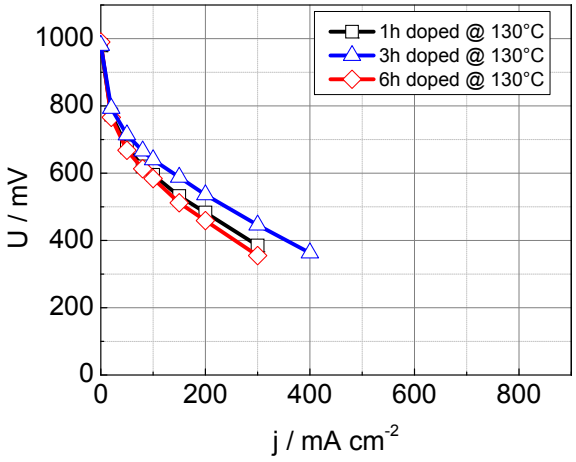

Fig. 6. Influence of the doping time of the AB-PBI membrane on the cell performance. Membranes were doped at 130 °C. T = 160 °C, A = 4 cm^2, 1 mg Pt cm^{-2}, hydrogen/air with λ = 1.4/2.

than twice as high as for membranes doped at 120 °C for 6 h. Membranes doped at 130 °C for either 1 or 6 h showed slightly higher membrane resistance and reduced fuel cell performance compared to 3 h doping time.

To determine the influence of the doping temperature on the fuel cell performance, MEAs based on membranes doped for 6 h at various temperatures were evaluated (Fig. 7). The MEA performance of membranes doped at 100 °C is lower than for 120 °C doping temperature due to an insufficient amount of phosphoric acid in the membrane. Doping temperatures above 120 °C lead to partially dissolution of the membrane and therefore drastically reduced cell performance. At 140 °C, most of the membrane samples exhibited holes and mechanical instability after the doping process.

Apparently the acid doping time and temperature have a significant influence on the doping level. But we note that the amount of phosphoric acid in the membrane alone does not completely determine the fuel cell performance. Doping time and temperature have to be optimised for each type of membrane to achieve the highest membrane conductivity and fuel cell performance. The best results for the fumapem AM cross-linked membrane were obtained by doping the membrane for 6 h at 120 °C.

3.4. Confocal Raman microscopy

Acid leaching can be reduced and membrane conductivity improved by a more homogenous distribution of phosphoric acid in the membrane which correlates with the distribution of interactions between phosphoric acid and the basic nitrogen (N)-sides of the AB-PBI. This can be investigated with confocal Raman microscopy which was used before for determining the distribution of bonded water in Nafion membranes [20]. There are also several publications on confocal Raman spectroscopy of pristine or phosphoric acid doped PBI-type polymers including PBI derivates [18,21–23].

Fig. 8 shows the Raman spectra of AB-PBI samples, either pristine (grey) or doped (pink) (in web version) for 6 h. The Raman shift relevant to this study is in the range from 750 to 2000 cm^{-1}. The measured Raman signals are in accordance with spectra shown in Ref. [21]. There, the AB-PBI samples were doped in a similar manner. For detailed assignments of the spectral peaks we therefore refer to Ref. [21]. The peaks at 1611 cm^{-1} and 1572 cm^{-1} from the phosphoric acid doped AB-PBI (highlighted area) were assigned to C=C/C=N benzimidazole ring stretching vibrations. They are

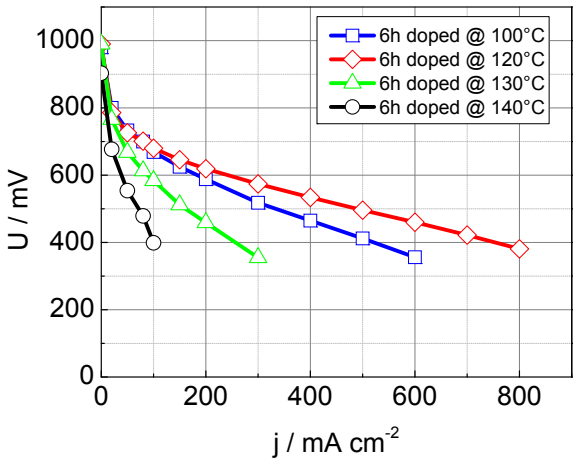

Fig. 7. Influence of the doping temperature of the AB-PBI membrane on the cell performance. Membranes were doped for 6 h. T = 160 °C, A = 4 cm^2, 1 mg Pt cm^{-2}, hydrogen/air with λ = 1.4/2.

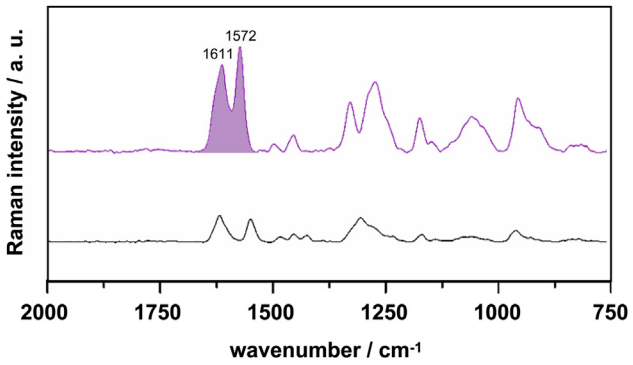

Fig. 8. Raman spectra of pristine (below) and 6 h doped (up) AB-PBI. Spectra were used for Raman mapping; red laser diode, λ = 785 nm, 50 mW output power, 20× objective, NA 0.45, integration times from 10 s to 30 s, at least four coadditons, spectral resolution 9 cm^{-1}.

associated with the formation of bonds between the acid protons of the phosphoric acid and the nitrogen atoms of the imidazole rings [30]. The peak intensity at 1572 cm^{-1} increases with increasing doping level whereas the peak at 1611 cm^{-1} remains almost constant. The integrated intensity of these two peaks (highlighted area) was used as an indicator for the interaction between AB-PBI host and phosphoric acid dopant and was therefore selected for creating the Raman maps.

Fig. 9 shows integrated Raman intensity maps with different doping times. The absolute intensities in Fig. 9 cannot be directly compared among the images due to different measurement conditions that were optimised for each sample. Hence only the relative intensity distributions are compared and discussed. Fig. 9a shows an inhomogeneous distribution after doping for just 1 h. The membrane is known to swell during the doping process [10], and we assume an initial physical acid uptake that takes place instantly after immersion in the hot phosphoric acid. The swelling process of the polymer due to the phosphoric acid uptake seems not to be finished at this point and therefore not all N-sides of AB-PBI are in contact with acid molecules. This can be correlated with the acid leaching effect and low conductivity observed for membranes doped at 120 °C for 1 h. After doping for 3 h patterns with larger uniform areas were observed (Fig. 9b). The increasing homogeneity of the phosphoric acid distribution with prolonged doping time is related to higher membrane conductivity and fuel cell performance.

The intensity distribution only slightly changed with prolonged doping time (Fig. 9c) which indicates that a steady state was established after 3 h. The ex-situ conductivity measurements also showed comparable values for membranes doped for 3 or 6 h at 120 °C, however the in-situ conductivity and the fuel cell performance were different. The Raman maps are limited to surface investigations and we assume that the changes in the phosphoric acid distribution proceed in the inner regions of the membrane with prolonged doping time. Storage overnight under dry conditions (Fig. 9d) has only a minor effect on the intensity distribution and results in a comparable cell performance.

We assume that the observed large areas in the Raman maps (Fig. 9c) with uniform intensity of the interactions between phosphoric acid and AB-PBI might be part of a superstructure. However further investigations are necessary to explain this observation and the possible correlation with the conductivity and fuel cell performance.

4. Conclusions

In this work, the effects of the doping time and temperature on the ex-situ and in-situ conductivities of phosphoric acid doped AB-

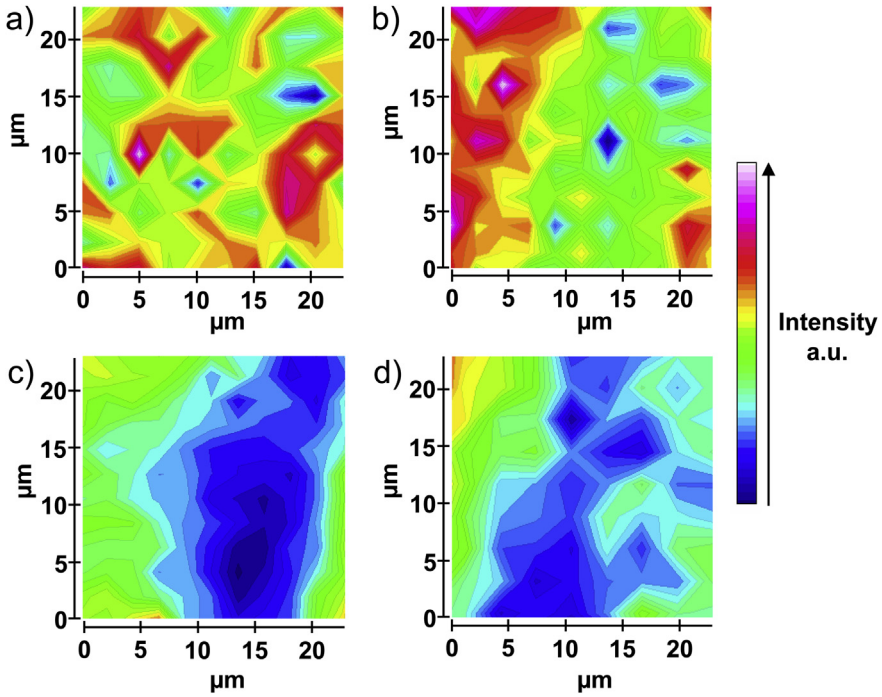

Fig. 9. Confocal Raman mapping of AB-PBI membranes with different doping times: a) 1 h, b) 3 h, c) 6 h, d) 6 h, dry storage over night. Side lengths in µm; absolute intensities are individual for each picture; red laser diode, $\lambda = 785$ nm, 50 mW output power, 20× objective, NA 0.45, integration times from 10 s to 30 s, at least four coadditons, spectral resolution 9 cm^{-1}.

PBI membranes and the fuel cell performance were investigated. The phosphoric acid distribution in the AB-PBI membranes at different doping levels was resolved with confocal Raman microscopy.

The doping time and temperature have a major impact on the in situ membrane conductivity and fuel cell performance not only due to the increased acid uptake with prolonged doping time but also because of a more uniform acid distribution through the membrane thickness. Therefore the imidazole groups of AB-PBI in the centre of the membrane are also in contact with phosphoric acid. Hydrogen bonds are formed between phosphoric acid protons and nitrogen atoms in this area. This results in increased membrane conductivity and prevents excessive acid migration from the membrane to the electrodes during fuel cell operation.

Confocal Raman microscopy allows us to visualize the spatial distribution of phosphoric acid in AB-PBI membranes, which supports the proposed model of interactions between phosphoric acid and the AB-PBI polymer during the doping process.

We assume that doping time and temperature have to be optimised for each type of membrane to achieve a sufficient amount of acid within the membrane though without deterioration of the mechanical stability of the membrane. However not only the amount of acid but also its distribution inside the membrane is crucial to achieve high membrane conductivity and fuel cell performance. The optimal parameters obtained in this study for fumapem AM cross-linked membranes were a doping time of 6 h and a doping temperature of 120 °C resulting in a doping level of 5.

Acknowledgments

We acknowledge the “Impuls- und Vernetzungsfonds der Helmholtz Gesellschaft” for the financial support (Young Investigator Group project VH-NG-616) and the “Zentrum für Sonnenenergie- und Wasserstoff-Forschung Baden-Württemberg“(ZSW) for providing the infrastructure.

References

[1] J.A. Asensio, E.M. Sánchez, P. Gómez-Romero, Chem. Soc. Rev. 39 (2010) 3210.
[2] J. Zhang, Z. Xie, J. Zhang, Y. Tang, C. Song, T. Navessin, Z. Shi, D. Song, H. Wang, D.P. Wilkinson, Z.-S. Liu, S. Holdcroft, J. Power Sources 160 (2006) 872.
[3] R. Borup, J. Meyers, B. Pivovar, Y.S. Kim, R. Mukundan, N. Garland, D. Myers, M. Wilson, F. Garzon, D. Wood, P. Zelenay, K. More, K. Stroh, T. Zawodzinski, J. Boncella, J.E. McGrath, M. Inaba, K. Miyatake, M. Hori, K. Ota, Z. Ogumi, S. Miyata, A. Nishikata, Z. Siroma, Y. Uchimoto, K. Yasuda, K. Kimijima, N. Iwashita, Chem. Rev. 107 (2007) 3904.
[4] C. Yang, P. Costamagna, S. Srinivasan, J. Benziger, A.B. Bocarsly, J. Power Sources 103 (2001) 1.
[5] S. Bose, T. Kuila, T.X.H. Nguyen, N.H. Kim, K. Lau, J.H. Lee, Prog. Polym. Sci. 36 (2011) 813.
[6] J.-T. Wang, R.F. Savinell, J. Wainright, M. Litt, H. Yu, Electrochim. Acta 41 (1996) 193.
[7] J.S. Wainright, J.-T. Wang, D. Weng, R.F. Savinell, M. Litt, J. Electrochem. Soc. 142 (1995) L121.
[8] Q. Li, R. He, J.O. Jensen, N.J. Bjerrum, Fuel Cells 4 (2004) 147.
[9] J. Lobato, P. Cañizares, M.A. Rodrigo, J.J. Linares, G. Manjavacas, J. Memb. Sci. 280 (2006) 351.
[10] R. He, Q. Li, A. Bach, J.O. Jensen, N.J. Bjerrum, J. Memb. Sci. 277 (2006) 38.
[11] J.S. Wainright, M.H. Litt, R.F. Savinell, in: Handbook Fuel Cells, John Wiley & Sons, Ltd, 2010.
[12] H.-J. Kim, S.Y. Cho, S.J. An, Y.C. Eun, J.-Y. Kim, H.-K. Yoon, H.-J. Kweon, K.H. Yew, Macromol. Rapid Commun. 25 (2004) 894.
[13] J.J. Linares, C. Sánches, V.A. Paganin, E.R. González, ECS Trans. 41 (2011) 1579.
[14] J. Asensio, J. Memb. Sci. 241 (2004) 89.
[15] B. Xing, O. Savadogo, J. New. Mater. Electrochem. Syst. 2 (1999) 95.
[16] Y.-L. Ma, J.S. Wainright, M.H. Litt, R.F. Savinell, J. Electrochem. Soc. 151 (2004) A8.
[17] L. Qingfeng, H.A. Hjuler, N.J. Bjerrum, J. Appl. Electrochem. 31 (2001) 773.
[18] Q. Li, R. He, R.W. Berg, H.A. Hjuler, N.J. Bjerrum, Solid State Ion. 168 (2004) 177.
[19] R.M. Silverstein, F.X. Webster, D.J. Kiemle, Spectrometric Identification of Organic Compounds, John Wiley & Sons, 2005.
[20] S. Deabate, G. Gebel, P. Huguet, A. Morin, G. Pourcelly, Energy Environ. Sci. 5 (2012) 8824.
[21] F. Conti, A. Majerus, V. Di Noto, C. Korte, W. Lehnert, D. Stolten, Phys. Chem. Chem. Phys. 14 (2012) 10022.
[22] E. Quartarone, A. Magistris, P. Mustarelli, S. Grandi, A. Carollo, G.Z. Zukowska, J.E. Garbarczyk, J.L. Nowinski, C. Gerbaldi, S. Bodoardo, Fuel Cells 9 (2009) 349.
[23] A. Sannigrahi, S. Ghosh, S. Maity, T. Jana, Polymer 51 (2010) 5929.
[24] F. Mack, M. Klages, J. Scholta, L. Jörissen, T. Morawietz, R. Hiesgen, D. Kramer, R. Zeis, J. Power Sources 255 (2014) 431.

[25] Q. Li, J.O. Jensen, C. Pan, V. Bandur, M.S. Nilsson, F. Schönberger, A. Chromik, M. Hein, T. Häring, J. Kerres, N.J. Bjerrum, Fuel Cells 8 (2008) 188.
[26] Y. Oono, A. Sounai, M. Hori, J. Power Sources 189 (2009) 943.
[27] Q. Li, J.O. Jensen, R.F. Savinell, N.J. Bjerrum, Prog. Polym. Sci. 34 (2009) 449.
[28] C. Wannek, W. Lehnert, J. Mergel, J. Power Sources 192 (2009) 258.
[29] F. Mack, T. Morawietz, R. Hiesgen, D. Kramer, R. Zeis, ECS Trans. 58 (2013) 881.
[30] G.A. Giffin, F. Conti, S. Lavina, A. Majerus, G. Pace, C. Korte, W. Lehnert, V. Di Noto, Int. J. Hydrogen Energy 39 (2014) 2776.